Time-resolved in-situ tomography for the analysis of evolving metal foam granulates

Authors

Francisco García-Moreno[ab]*, Paul H. Kamm[a], Tillmann R. Neu[a] and John Banhart[ab]

[a] Helmholtz-Zentrum Berlin für Materialien und Energie, Hahn-Meitner-Platz 1, Berlin, 14109, Germany

[b] Technische Universität Berlin, Hardenbergstr. 36, Berlin, 10623, Germany

Correspondence email: garcia-moreno@helmholtz-berlin.de

Synopsis Setup for time-resolved in-situ tomography with up to 25 tomographies per second is implemented at the EDDI beamline, BESSY II, Germany. The capabilities of the methods are demonstrated by analysing the foaming behaviour of a metallic foam granulate.

Abstract An experimental setup has been developed that allows for capturing up to 25 tomograms per second using the white X-ray beam at the experimental station EDDI of BESSY II, Berlin, Germany. The key points are the use of a newly developed, precise and fast rotation stage, a very efficient scintillator and a fast CMOS camera. As a first application, the foaming of aluminium alloy granules at 650 °C is investigated in-situ. Formation and growth of bubbles in the liquid material are observed and found to be influenced by the limited thermal conductivity in the bulk of granules. Changes that take place between two tomographic frames separated in time by 39 ms can be detected and analysed quantitatively.

Keywords: Tomography, time-resolved, in-situ, dynamic processes, metal foam, granulates

1. Introduction

Dynamic processes in evolving metallic foams have been studied in-situ using fast X-ray radioscopy (Garcia-Moreno *et al.*, 2008, Rack *et al.*, 2009, Garcia-Moreno *et al.*, 2012). Although acquisition rates over 100,000 fps have been reached (Garcia-Moreno *et al.*, 2012) and valuable insights into the dynamics of foaming and the corresponding morphological changes in foams were gained, radiographic information is often ambiguous and limited to flat sample configurations. In-situ tomography lifts some of the restrictions but has been too slow for real-time studies.

Recent developments have led to higher temporal resolutions through improved instrument hardware and data processing capabilities. That acquisition times are becoming shorter is mainly due to the use of high-brilliance 3rd generation synchrotron sources, highly efficient scintillators and improved optics. As a consequence, fast tomography with up to 20 tomographies per second (20 Hz) has

become available at different beamlines (Rack *et al.*, 2010, Momose *et al.*, 2011, Takano *et al.*, 2013, Mokso *et al.*, 2015, Maire *et al.*, 2016, Kamm *et al.*, 2017, dos Santos Rolo *et al.*, 2014, Lovric *et al.*, 2016). Evolving metallic foams (García-Moreno *et al.*, 2013, Jiménez *et al.*, 2018, Kamm *et al.*, 2017) can now be studied in real time with in-situ tomography. Furthermore, operando studies such as cycling of rechargeable batteries (Schröder *et al.*, 2016) or operating fuel cells (Alrwashdeh *et al.*, 2017) are currently in the focus of research.

In this work, we present the latest development in imaging acquisition speed at the EDDI beamline at BESSY II, Berlin, Germany, where we are now able to perform time-resolved in-situ tomography up to 25 Hz, which is the fastest tomography acquisition rate reported at synchrotrons so far. As a case study we analyse the foaming behaviour of a metallic foam granulate. Similar to polymeric foams, use of expandable granulates is interesting from the application point of view. As the surface-to-volume ratio of granules compared to standard bulk precursors is much larger, their foaming behaviour might suffer from insufficient gas nucleation or increased gas losses, incomplete particle bonding and result in non-uniform pore sizes and foam densities (Duarte *et al.*, 2013, Nosko *et al.*, 2010). Therefore we study the foaming behaviour of single granulates and the time-resolved bubble size evolution.

2. Experimental procedure

A new high-speed rotation stage (see Fig. 1) jointly developed at the Helmholtz-Zentrum Berlin and the Technische Universität Berlin is used. Here, it is applied to explore fast phenomena in evolving metal foams with a rotation frequency of ~12.5 Hz, which allows us to capture tomographies with ~25 Hz, each of which requires a rotation by 180°. The stage features a precision rotation axis with ball bearings and a servo drive regulated by an angular PID speed controller with sensor feedback from the servo drive, programmable by a self-developed Labview-based software. No electric sliding contacts for the rotation system are available, which is why heating and temperature measurement are conducted contactless. Special attention has been paid to centring samples and crucibles precisely as no xy table was used and centrifugal forces reach 0.6 g at the inner side of the crucible of radius r_i ~1 mm.

AlSi10 + 0.5 TiH_2 (all in wt.%) foamable precursor granulate of equivalent diameter ~1 mm is produced following the powder metallurgical route described elsewhere (Banhart, 2006). The granules are placed in an X-ray transparent boron nitride (BN) crucible of 2.2 mm inner and 3 mm outer diameter. Foaming is induced by heating the samples in the crucible with a ramp of ~2 K/s to around 650 °C by a 150 W IR lamp (Osram, Germany) from the top (see Fig. 1). Foaming starts during the heating phase at around 580 °C close to the eutectic temperature of the Al-Si alloy (577°C) when the system is not under isothermal conditions.

A white X-ray beam (about 6–120 keV) is provided by a superconducting 7 T multipole wiggler. A 200-µm thick LuAG:Ce scintillator is used to convert the transmitted images into visible light, after

which a mirror projects the light onto a PCO Dimax CMOS camera. A more detailed explanation of the imaging system can be found elsewhere (Jiménez *et al.*, 2018, García-Moreno *et al.*, 2013).

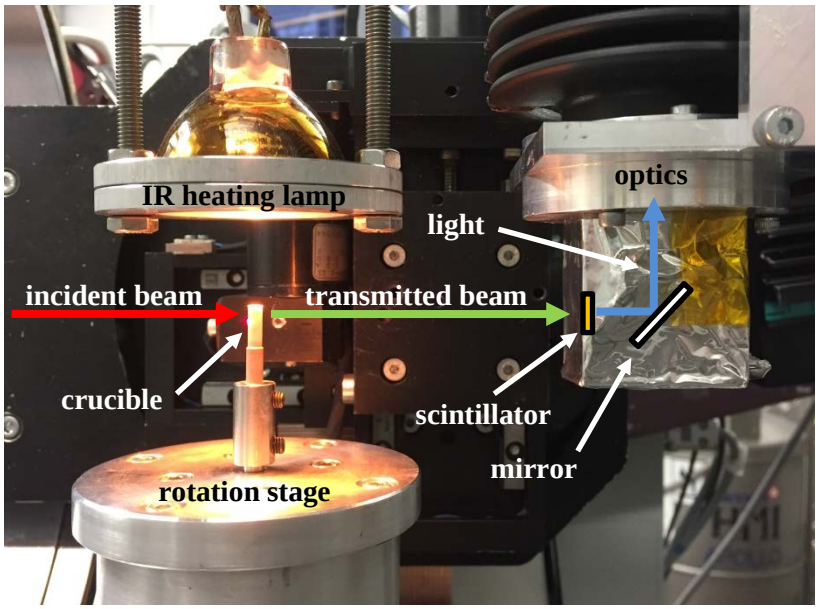

Figure 1 Time-resolved in-situ tomography setup installed at the EDDI instrument and composed of a fast rotation stage, an IR heating lamp (temperature up to 800 °C), an X-ray transparent BN crucible, a 200-µm thick LuAG:Ce scintillator, a white beam optical system configuration and a PCO Dimax CMOS camera. The incident (red), and transmitted (green) X-ray beams as well as the light path from the scintillator to the camera (blue) are given.

A compromise between pixel size, field of view (FOV), number of projections and rotation speed is necessary depending on the experiment type and requirements. In the present case, the acquisition parameters are: a spatial resolution of 5 µm measured on a micro resolution test pattern from JIMA, Japan, a FOV of 3.44 mm × 1.85 mm (given by the pixel size of 2.5 µm), an exposure time of 0.48 ms for each single projection, 78 projections per tomography (sufficient for our purpose), and a time resolution of ~39 ms per tomography. The Common Unified Device Architecture (CUDA)-accelerated filtered back-projection (FBP)-algorithm-based reconstruction is performed using the open source ASTRA Toolbox (van Aarle *et al.*, 2016). Tomographies with 25.6 Hz are acquired throughout 15.5 s.

3. Results and discussion

396 tomograms are acquired in ~15.5 s to follow the stage of gas nucleation and subsequent bubble evolution in AlSi10 + 0.5 TiH_2 granules as they are heated. The high rate of ~25 Hz allows us to resolve in-situ and in detail the bubble evolution inside each single granule. Fig. 2c) shows six xy-slices at a particular height (z = 1.4 mm) extracted from the series of 396 tomograms. Nucleation

probably starts around $t \approx 0$ s in the granule at the lower right, but in fact we only observe bubble growth in early stages because nucleation itself is not observable due to insufficient spatial resolution. Pores of 1-2 µm diameter contribute most to the total bubble volume in the nucleation stage of Zn foams as measured by neutron scattering but pores as small as 50 nm could be also detected. (Banhart *et al.*, 2001). We assume that each appearing bubble corresponds to a single nucleus (Kamm *et al.*, 2017). At $t \approx 2.5$ s the second granule (lower left) and at $t \approx 5$ s the third one (middle) follow as manifested by the appearance of the first bubbles. The different onset times are understandable because the heat applied is transmitted into the grains from the direction of the heating lamp and through the crucible walls and there is a small radial and a larger axial temperature gradient inside the crucible. Moreover, intergranular heat transfer is low because of the small contact area between granules, which leads to a slight temperature delay in some particles depending on their location. This observation underlines a difference to bulk samples and can explain the varying pore sizes and densities of solidified foams made from granules reported in the literature (Nosko *et al.*, 2010). On the other hand, intragranular nucleation takes place almost simultaneously due to good heat transfer within individual granules as in bulk samples (Kamm *et al.*, 2017).

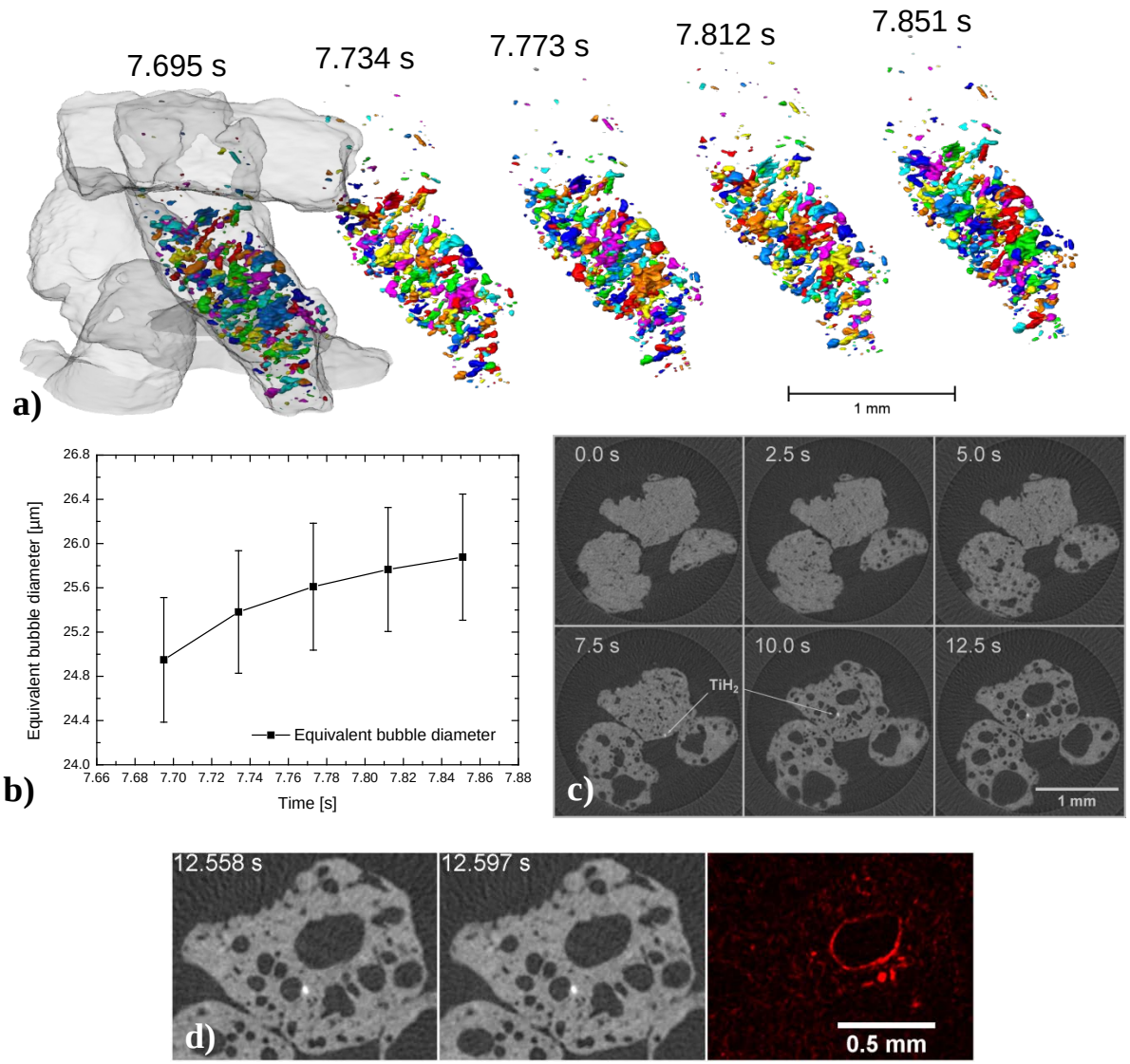

Figure 2 Time-resolved tomography (~25 Hz) of AlSi10 + 0.5 wt.% TiH_2 precursor granules foaming at ~650 °C in a cylindrical BN crucible. a) Tomogram of several granules at t = 7.695 s with bubbles coloured for the central granule, and time evolution of the bubbles in this granule over 5 tomographies separated each by only 39 ms. b) Time evolution of the mean equivalent bubble diameter over 156 ms corresponding to a). c) Series of six 2D slices separated by 2.5 s each as extracted from the series recorded over 15.5 s during foaming, and showing the appearance and growth of gas bubbles and foam evolution. Small white dots correspond to TiH_2 particles. d) Two 2D slices of one granule at t = 12.558 s and t = 12.597 s and the corresponding difference image showing changes in red.

The tomogram at t = 7.695 s shown in Fig. 2a) as a 3D rendering features several granules in transparent grey and a selected grain with individual bubbles internally highlighted by different colours as obtained by binarisation and segmentation of the image. It also shows the same single granule again four times more within time intervals of 39 ms, i.e. at t = 7.734 s, 7.773 s, 7.812 s and

7.851 s, thus exploiting the maximal temporal resolution of our experiment. This visual comparison together with the corresponding analysis of the mean value of the equivalent diameters of all bubbles (Fig. 2b) reveals the changes in bubble size and distribution within these very small time intervals. This result underlines the highly dynamic nature of foaming although the difference in this short period is smaller than the standard error of the mean diameters. The number of bubbles remains nearly constant at 1298 ± 24 between t = 7.695 s and t = 7.851 s, suggesting that already at this early foaming stage there is no more nucleation or a balance between newly appearing bubbles and those that already start to merge or disappear. The foam bubble evolution at a later stage (t = 12.558 s and t = 12.597 s) is depicted in Fig. 2d), where the difference image shows in red changes between the two slices, e.g. shrinkage of the central bubble and rupture of a smaller one, thus emphasising the need of such high spatio-temporal resolution.

4. Conclusions

Time-resolved tomography up to 25.6 Hz is now available and a powerful characterisation tool for in-situ analyses in material science.

Granules of AlSi10 alloy + TiH_2 of ~1 mm equivalent diameter are foamed and their foaming sequence is found to be dependent on their position. This can be explained by an inferior intergranular thermal contact, although intragranular bubble size evolution is found to be comparable to that of bulk precursors.

The distribution of equivalent bubble size diameters and its mean value evolve even in the short time between two tomograms (39 ms), thus emphasising the need for high temporal resolution.

Acknowledgements Funding by the European Space Agency (project AO-99-075) and German Research Foundation (project BA 1170/35-1 and GA 1304/5-1) is gratefully acknowledged.

References

Alrwashdeh, S. S., Manke, I., Markötter, H., Haußmann, J., Arlt, T., Hilger, A., Al-Falahat, A. M., Klages, M., Scholta, J. & Banhart, J. (2017). *Energy Technology* **5**, 1612-1618.
Banhart, J. (2006). *Adv. Eng. Mater.* **8**, 781-794.
Banhart, J., Bellmann, D. & Clemens, H. (2001). *Acta Mater.* **49**, 3409-3420.
dos Santos Rolo, T., Ershov, A., van de Kamp, T. & Baumbach, T. (2014). *Proceedings of the National Academy of Sciences* **111**, 3921-3926.
Duarte, I., Oliveira, M., Garcia-Moreno, F., Mukherjee, M. & Banhart, J. (2013). *Colloids Surf., A* **438**, 47-55.
García-Moreno, F., Jimenez, C., Kamm, P. H., Klaus, M., Wagener, G., Banhart, J. & Genzel, C. (2013). *J. Synchrotron Rad.* **20**, 809-810.
Garcia-Moreno, F., Mukherjee, M., Jiménez, C., Rack, A. & Banhart, J. (2012). *Metals* **2**, 10-21.
Garcia-Moreno, F., Rack, A., Helfen, L., Baumbach, T., Zabler, S., Babcsan, N., Banhart, J., Martin, T., Ponchut, C. & Di Michiel, M. (2008). *Appl. Phys. Lett.* **92**, 3.
Jiménez, C., Kamm, P. H., Plaepow, M., Neu, T., Klaus, M., Wagner, G., Banhart, J., Genzel, C. & García-Moreno, F. (2018). *J. Synchrotron Rad.* **submitted**.

Kamm, P. H., García-Moreno, F., Neu, T. R., Heim, K., Mokso, R. & Banhart, J. (2017). *Adv. Eng. Mater*. **19**, 1600550-n/a.
Lovric, G., Mokso, R., Schlepütz, C. M. & Stampanoni, M. (2016). *Physica Med.* **32**, 1771-1778.
Maire, E., Le Bourlot, C., Adrien, J., Mortensen, A. & Mokso, R. (2016). *Int. J. Fract.* **200**, 3-12.
Mokso, R., Schwyn, D. A., Walker, S. M., Doube, M., Wicklein, M., Müller, T., Stampanoni, M., Taylor, G. K. & Krapp, H. G. (2015). *Sci. Rep.* **5**, 8727.
Momose, A., Yashiro, W., Harasse, S. & Kuwabara, H. (2011). *Opt. Express* **19**, 8423-8432.
Nosko, M., Simančík, F. & Florek, R. (2010). *Materials Science and Engineering: A* **527**, 5900-5908.
Rack, A., Garcia-Moreno, F., Baumbach, T. & Banhart, J. (2009). *J. Synchrotron Rad.* **16**, 432-434.
Rack, A., Garcia-Moreno, F., Schmitt, C., Betz, O., Cecilia, A., Ershov, A., Rack, T., Banhart, J. & Zabler, S. (2010). *J. Xray Sci. Technol.* **18**, 429-441.
Schröder, D., Bender, C., Arlt, T., Osenberg, M., Hilger, A., Risse, S., Ballauff, M., Manke, I. & Janek, J. (2016). *J. Phys. D: Appl. Phys.* **49**, 404001.
Takano, H., Morikawa, M., Konishi, S., Azuma, H., Shimomura, S., Tsusaka, Y., Nakano, S., Kosaka, N., Yamamoto, K. & Kagoshima, Y. (2013). *J. Phys. Conf. Ser.* **463**, 012025.
van Aarle, W., Palenstijn, W. J., Cant, J., Janssens, E., Bleichrodt, F., Dabravolski, A., De Beenhouwer, J., Joost Batenburg, K. & Sijbers, J. (2016). *Opt. Express* **24**, 25129-25147.

Supplements

A – Video of xy-slices time evolution at a particular height (z = 1.4 mm) extracted from the series of 396 tomograms.